

BEAM-PARK EXPERIMENT 1/2000: RESULTS AND COMPARISON WITH MASTER/PROOF'99

D. Banka⁽¹⁾, R. Jehn⁽²⁾, L. Leushacke⁽¹⁾, and J. Rosebrock⁽¹⁾

⁽¹⁾*Research Institute for High Frequency Physics and Radar Techniques (FHR) in FGAN,*

⁽¹⁾*Neuenahrer Str. 20, D-53343 Wachtberg, Germany, Email: Banka@fgan.de*

⁽²⁾*European Space Operations Centre (ESOC),*

⁽²⁾*Robert-Bosch-Str. 5, D-64293 Darmstadt, Germany, Email: Ruediger.Jehn@esa.int*

ABSTRACT

A monostatic 24-h debris observation campaign (BPE-1/00) has been prepared and conducted using FGAN's TIRA L-Band system. Based on experiences from previous beam-park experiments a similar largely automated data processing is applied on an extended range window of 300 – 2000 km. More than 1500 detections are encountered, 471 of them are verified as being real targets in Low-Earth-Orbit (LEO). In comparison with previous experiments the statistics show similarities confirming the concept of beam-park experiments for space debris observations, despite the snapshot character of 24-h experiments. The comparison with MASTER/PROOF'99 and ORDEM2000 leads to a reasonable agreement between models and observations.

Key words: Beam-park experiment; space debris population; space debris situation; MASTER; PROOF; radar.

1. INTRODUCTION

The space debris situation is highly dynamic mainly due to a number of on-orbit break-ups per year and several debris producing events per month. The observation of this environment can be performed by optical or radar means.

Ideally the whole volume of LEO should be observed at a single point in time to obtain the most complete picture of the space debris situation possible. Realistically one has to find a balance between sensitivity and the size of the observation volume. To achieve the capability of detecting objects of down to 1-cm size in LEO most sensors are limited to a pencil shaped observation volume of less than 1° width. To increase the size of the total observation volume several millions of those single observations are performed in one experiment (One single observation corresponds to one pulse record in radar terms). This pencil-shaped observation volume is kept fixed (by 'parking' the antenna) and the Earth's rotation is used to move the radar beam through LEO, leading to beam-park experiments. For one revolution of the Earth (24 h) in this setup the beam follows approximately the circumference of a truncated cone. Application of several sensors at different latitudes offers another increment of

the observation volume. To achieve this, several sensors are usually internationally co-ordinated. Radar systems can operate independently from weather and time leading to uninterrupted 24-h campaigns. Optical systems participate by accumulating observation time during several sunsets/-rises.

24-h beam-park experiments can only record a snapshot of the debris situation which necessitates frequent observation campaigns with ground based sensors. The most recent campaign was carried out during the last week of October 2000. FGAN participated with its TIRA L-Band monopulse system exploiting an extended data acquisition system, allowing a range window of 300 – 2000 km, and thus covering all LEO altitudes for the first time with TIRA.

2. EXPERIMENT

At FGAN the beam-park experiment BPE-1/00 started on Oct 27th, 2000 at 11:58 UT and ended at 12:09 UT on the next day. From the position at 50.6166° N and 7.1296° E (293 m above sea level) TIRA's antenna pointed eastwards with an elevation of 75°. This gives a nearly unambiguous relationship between the measured Doppler frequency shift and the object's orbit inclination if a circular orbit is assumed. At 1.333 GHz centre frequency the 3dB-beamwidth of the 4-horn monopulse system is 0.5°. The noise equivalent radar cross section (RCS) at 1000 km range is -48 dBsm corresponding to 2 cm object size. A 1-ms pulse length was used with a repetition period of 29 ms and a peak power of mostly 1.5 MW.

Before and after the experiment the radar system was calibrated by tracking satellites 22875 (2-m sphere; COSMOS-2265) and 6212 (cylinder with elliptical end caps; RADCAT) respectively. Both calibration experiments resulted in the same calibration factor.

Some minor failures caused a total loss of data for about 8 min, but this is compensated for by additional 12 min of observation time. In total 240 Gb of data in three channels (sum, elevation difference and traverse difference) were acquired. More details on TIRA and the data collection units can be obtained from [1].

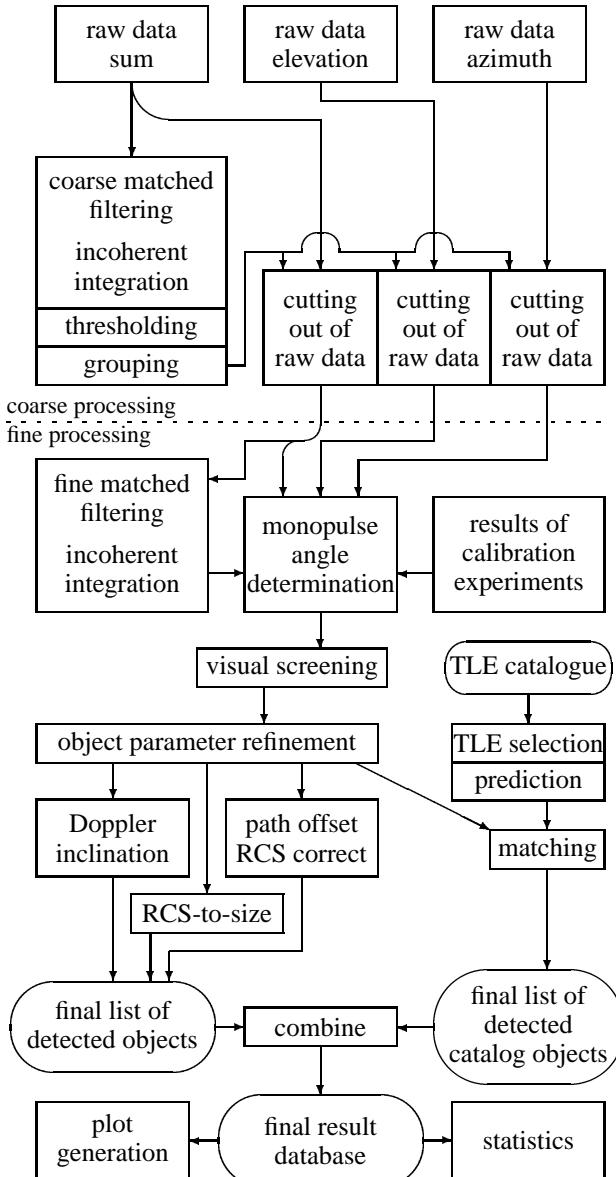


Figure 1. Processing flow chart.

3. DATA PROCESSING

The largely automated processing is based on the same routines as the ones used for the previous beam-park experiments ([1], see Fig. 1).

The coarse processing finds groups of pulse records which might contain reflections from one or more real objects. The raw data of these groups are fine-processed resulting in information on range, range rate and signal-to-noise ratio (SNR) for every echo in each record. In a next step those echos around a fixed range/range-rate cell are combined into detections of possible objects spanning several records. Range, range rate and SNR get related to a detection at the closest point of approach (CPA) to the radar-line of sight. A manual screening process works on these detections and distinguishes single real objects

Table 1. BPE-1/00; Processing results.

coarse processing finds 1578 groups 1528 groups go into visual screening process	
real objects	22 %
multiple objects	3 %
leading to 1577 datasets after separation extended range detections	1 %
ionospheric reflections and implausible parameters	74 %
No. of objects detected	471
catalogued objects	94

from several objects in the beam (to be separated manually), from extended range detections (excluded for not being part of LEO), and from ionospheric reflections or 'objects' with implausible parameters (rejected). The result of this selection process is shown in Tab. 1.

As a last processing step the detections are checked against the USSPACECOM SSN two-line element (TLE) catalogue. TLE sets closest to the experiment date are chosen and objects unobservable due to geometrical constraints (e.g. GEO objects, objects of low inclination) are excluded. Of the remaining ones an orbit propagator determines all objects, which should have been detected by TIRA in a hypothetical 10°-radar beam. This list is matched with the detections of the experiment by applying the following thresholds for the differences: Time < 3 s, angle < 0.5°, range < 10 km and range rate < 0.3 km/s. This check also confirms extended range detections — four in BPE-1/00 —, leaving 471 detections in LEO of which 94 are catalogued with TLE sets.

The Program for Radar and Optical Observation Forecasting (PROOF'99; [2]) in conjunction with TLE sets of the catalogue population dated Oct 25th, 2000 predicted deterministically 120 catalogue objects to be seen during the experiment with TIRA. Nearly 2/3 of them are confirmed by the experiment.

4. RESULTS

In Fig. 2 objects' altitudes are evenly distributed over time confirming the idea of the experiment as described in the introduction. This also means that observing with optical telescopes for only a few hours per day during sunset-/rise provides unbiased data which can be used for general statistical analysis. However, this even distribution cannot be generalized for all times. The Cooperative Beam-Park Experiment COBEAM-1/96 [3] showed clustering in time due to the Pegasus/HAPS explosion 5 months before. Fig. 2 also reveals the densely populated altitude belts at 900 – 1000 km and around 1400 km (see the pronounced peaks in Fig. 10).

A similar picture is given in Fig. 3: In BPE-1/00 the Doppler-inclinations do not cluster in time, with the main

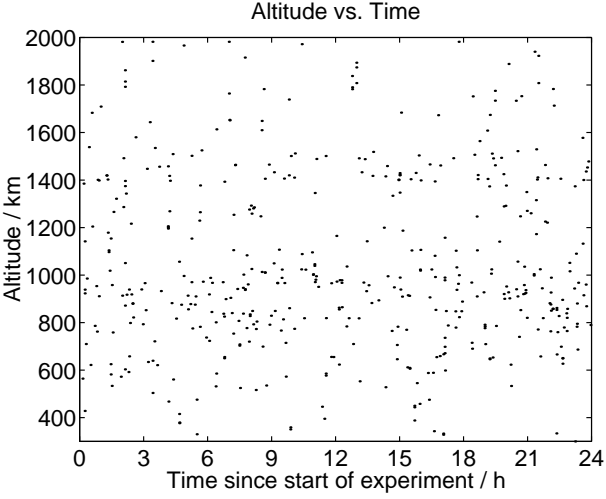


Figure 2. BPE-1/00: Distribution of altitudes vs. time.

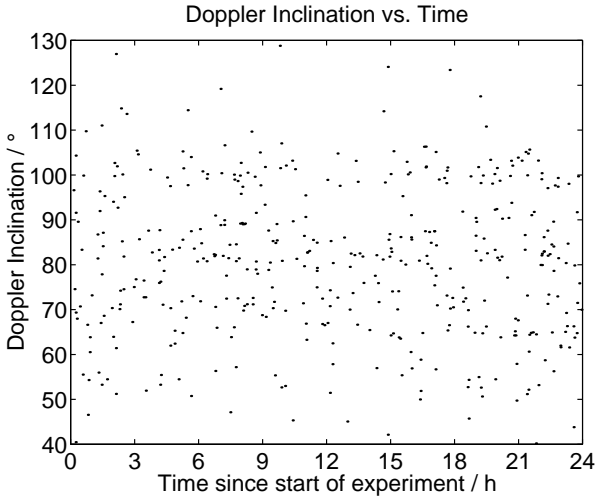


Figure 3. BPE-1/00: Distribution of Doppler inclinations vs. time.

belts around 70° , 80° and 100° (see also Fig. 9). Objects outside of the possible inclination interval between 50° and 130° are due to higher eccentricities, because the model of converting range rates (i. e. Doppler shifts) into inclinations assumes circular orbits. This assumption holds in many but not all cases, as shown in Fig. 4 for the detected catalogued objects: The inclination of objects of low eccentricity, i. e. (nearly) circular orbits is confirmed by the observation applying this conversion model. Large differences between the inclination of an object's TLE set and its inclination determined via the Doppler shift are associated with higher eccentricities.

Fig. 5 combines Fig. 2 and Fig. 3, and it shows the known clusters at e. g. 65° , 920 km or the Globalstar constellation orbit at around 55° , 1400 km [4]. The decreasing sensitivity with altitude/range is demonstrated by Fig. 6. The calibrated RCS is converted to a sphere equivalent object diameter with the help of NASA's size estimation model (SEM; [5]).

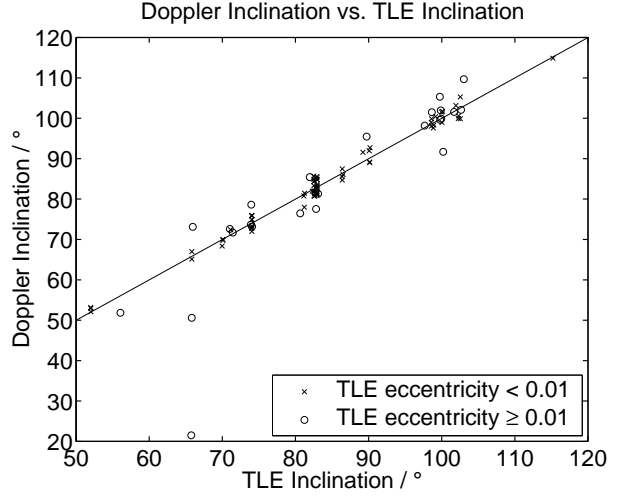


Figure 4. BPE-1/00: Distribution of Doppler inclination vs. TLE inclination for detected catalogue objects.

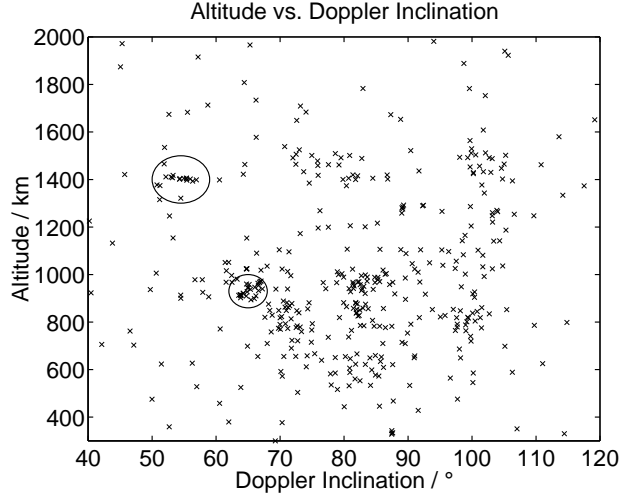


Figure 5. BPE-1/00: Distribution of altitudes vs. Doppler inclination.

Up to this point the distribution of objects crossing the single 0.5° -radar beam during the 24-h experiment is considered, leaving us with a very limited observation volume and a small probability that an object is actually detected. A statistical extrapolation into the entire volume of LEO is made by considering a random distribution of ascending nodes and true anomalies, but keeping the information on inclination and sensitivity. Fig. 7 shows confidence intervals for the total number of detectable objects in 50-km-altitude bins. To generate this diagram, first the probability of a randomly distributed object (with respect to the ascending node and the true anomaly) to cross TIRA's radar beam is calculated, yielding to a value on the order of 1 % during a 24-h campaign. On the basis of an inclination distribution taken from the 2-cm population of the CNUCE orbital debris reference model (CODRM99) and a binomial distribution, which is approximated by a Gaussian distribution, this probability is inverted and a 99%-confidence interval calculated (for

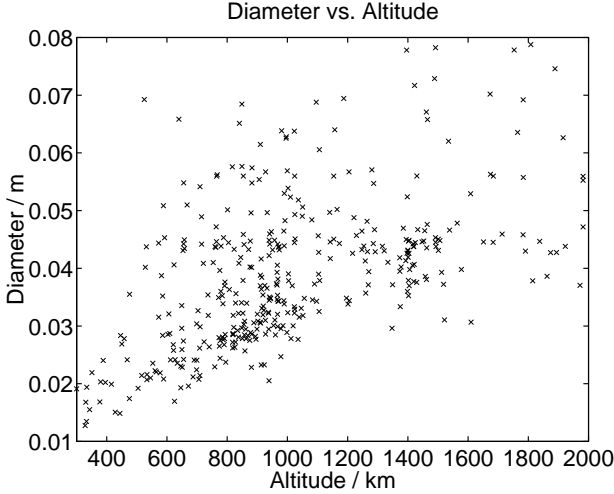


Figure 6. BPE-1/00: Distribution of RCS-equivalent-diameter vs. altitude.

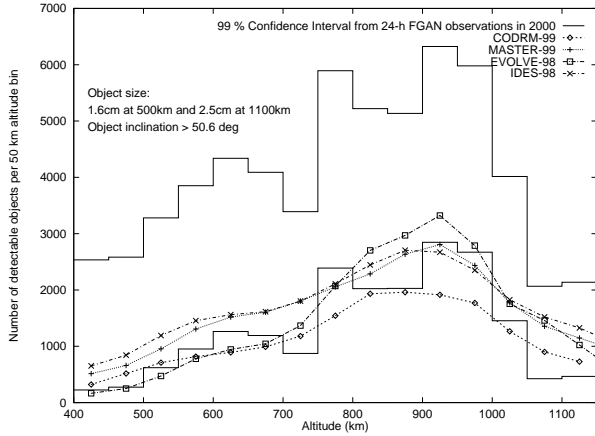


Figure 7. BPE-1/00: The two step curves show the confidence interval for the number of objects which can be detected with the FGAN radar. The lines with markers give this number as predicted by four different space debris models.

details see [6]). In the same figure the number of detectable objects (fulfilling the constraints on inclination and sensitivity) is shown as predicted by CODRM99, the ESA MASTER model, the NASA EVOLVE model and the DERA IDES model. The general altitude dependence is confirmed. Nonetheless the models are at the lower end or even below the confidence interval.

5. CHANGES OF THE SPACE DEBRIS SITUATION

From a comparison between the statistical results of BPE-1/00 and the ones of the beam-park experiments in February and April 99 some changes of the space debris situation might be recognized. In Fig. 8 and Fig. 9 the arithmetic mean of both the previous experiments is shown in relation to the results of BPE-1/00. The general similarity in Fig. 8 confirms the reproducibility of beam-park

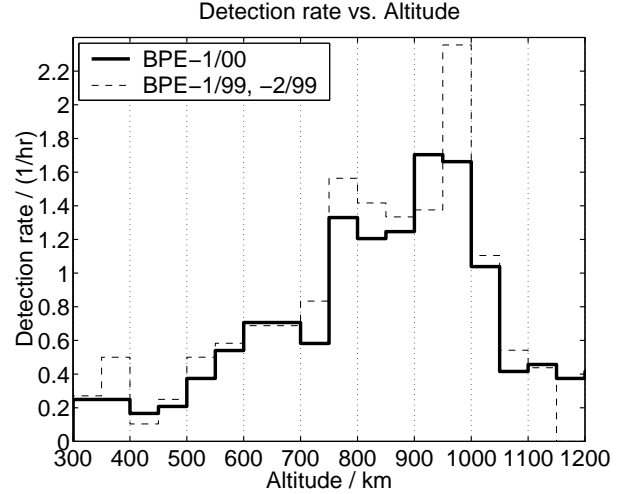


Figure 8. Hourly detection rates vs. altitude, 50-km bins.

experiments beyond their snapshot character. The most obvious change can be recognized in the 950 – 1000-km-altitude bin. The combination with the 900 – 950-km bin leads to the assumption a significant number of objects moved downwards, most likely debris objects due to their orbital decay. The differences between 700 and 850 km altitude are considered being inside statistical error margins. Debris objects lower than 400 km would have left LEO entirely in the course of the 18 months between the experiments.

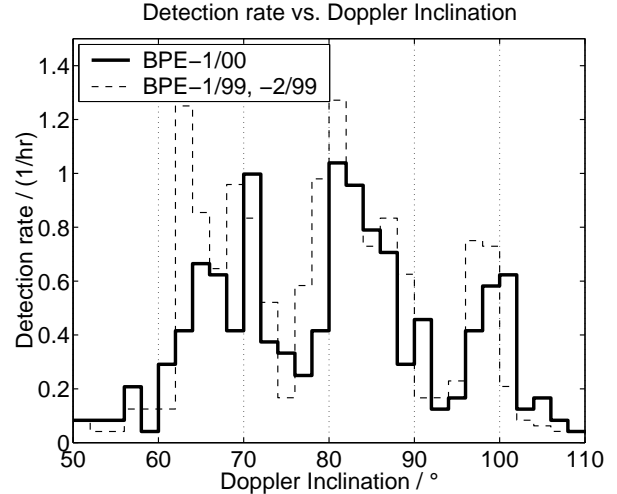


Figure 9. Hourly detection rates vs. doppler inclination of objects closer than 1200 km, 2° bins.

Fig. 9 shows the corresponding general similarity in inclination derived from the Doppler frequency. To be comparable with the previous experiments (and Fig. 8) only objects closer than 1200 km are considered. Differences might be related to statistical uncertainties. Major discrepancies still have to be clarified.

6. COMPARISON WITH ORBITAL DEBRIS DISTRIBUTION MODELS

For risk assessments of satellites, models to describe the orbital debris environment are widely used. The Meteoroid and Space Debris Terrestrial Environment Reference (MASTER; [7]) uses PROOF [2] to validate its debris model. NASA's Orbital Debris Engineering Model ORDEM2000 [8] has its own radar assessment routine providing debris fluxes in 50-km-range bins.

Table 2. Parameter for TIRA used in PROOF.

Beamwidth (radar FOV)	0.5°
Wavelength	0.225 m
Pulse repetition period	29.0 ms
NRCS Noise equivalent RCS	-48.0 dB
Transmitted power	1.50 MW
Pulse duration	1.0 ms
Range (NRCS)	1000.0 km
Desired false alarm time	10 h
No. threshold decisions per pulse	3300.0
Max. number of pulses to integrate	65
Geographic latitude	50.6166°
Geographic longitude	7.1296°
Altitude	293 m
Max. Range	2000.0 km
Min. Range	300.0 km
Azimuth	90°
Elevation	75°

A more detailed comparison is given in Fig. 10 – 13. For this comparison PROOF is run with parameters for TIRA shown in Tab. 2). To reduce fluctuation effects due to small objects with high representation factors, three runs with different random generator seed values are executed, and the mean of the results is used for the diagrams. The mean number of modelled detections is 276, only 58.6 % of 471 detected objects (Tab. 1).

In Fig. 10 the results of a calculation with ORDEM2k is included. ORDEM2k's output consists of a table of surface area fluxes, which are to be set in some relation to a 'surface' of the beam. Here a rectangular surface was chosen with the height of a range bin and the width equal to the width of the 3-dB beam in the middle of the range bin considered. This simple approximation involves errors of complicated origin, which are accounted for by PROOF when using MASTER. The model detection rate of objects larger than 1 cm is shown, but a range dependent detection rate for BPE-1/00 has to be kept in mind.

The comparison of the observation with the models reveals similarities in terms of the graphs' shape, and an underestimation of the observation by the models. The altitude regions between 1050 km and 1400 km and above 1600 km can be considered being modelled inside the error margins, but the peaks i. e. the heavily populated orbits are underestimated significantly. Due to the lower size limit ORDEM2k models the altitude range between

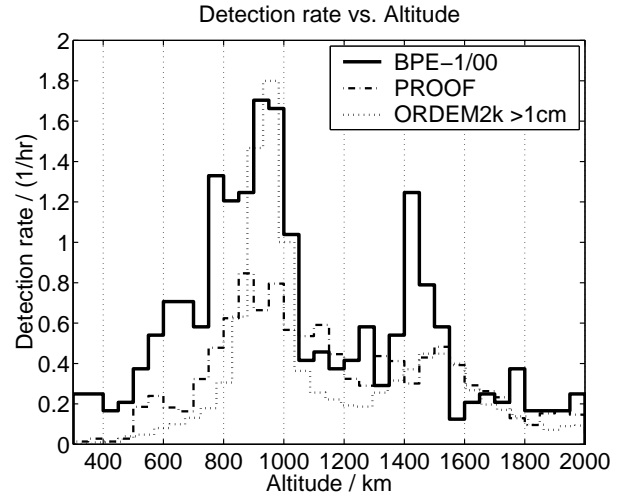


Figure 10. Hourly detection rates vs. altitude, 50-km bins. For ORDEM2k the class of objects larger 1 cm is used.

900 and 1000 km satisfactorily, but this detection rate is reached through observation by considering objects larger than 2 cm only. The sharp peak at 1400 km is missing in both models.

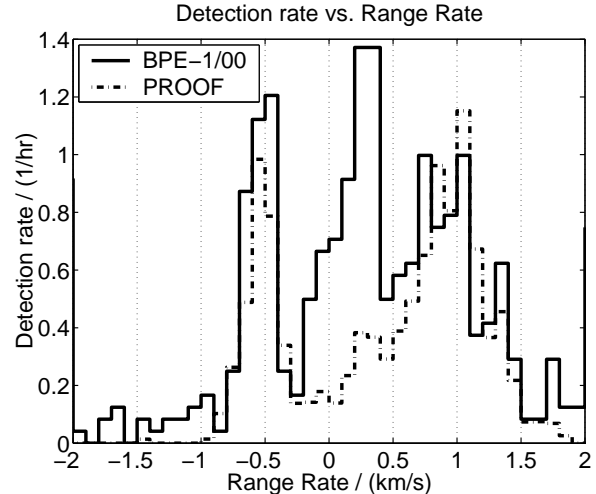


Figure 11. Hourly detection rates vs. range rate, 0.1-km/s bins.

In Fig. 11 a good agreement between the model and the observation can be seen for two maxima (around -0.5 km/s and around 1 km/s range rate). The peak between 0 and 0.5 km/s is not modelled. Because the Doppler inclination is closely related to range rate, a similar picture is expected in Fig. 12. But it shows differences by overestimating inclination intervals between 60° and 70° and underestimating the interval between 76° and 98° as well as 50° to 58°. The peak around 100° can be considered as being modelled correctly. The difference in the peaks in Figs. 11 and 12 can be explained by the altitude dependence of the Doppler inclination algorithm and by the numerous non-zero eccentricity orbits. The overestimation between 60° and 70° is associated with

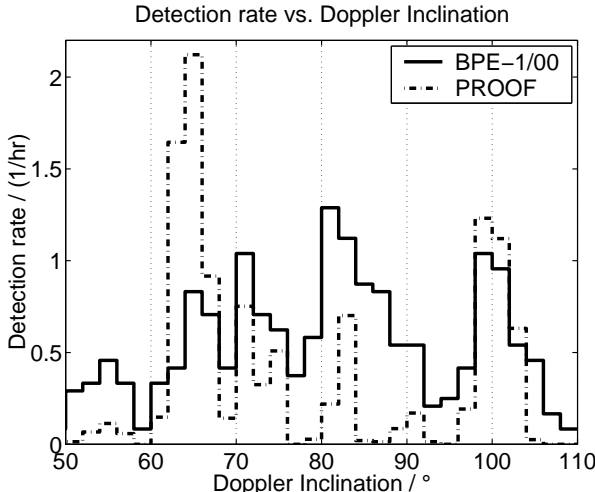


Figure 12. Hourly detection rates vs. Doppler inclination, 2° bins.

elliptical orbits of the 65° -population. The orbits of 2/3 of this model population have eccentricities higher than 0.01. Those objects - if observed - are spread over several bins in the detection rate vs. Doppler inclination diagram (Fig. 12) of the observed objects.

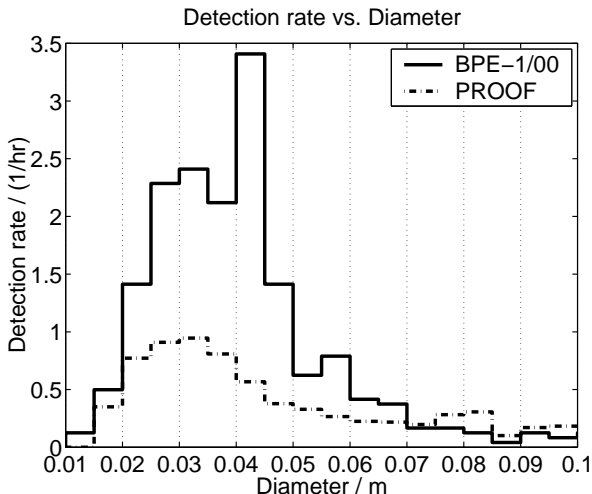


Figure 13. Hourly detection rates vs. RCS-equivalent-diameter, 0.5-cm bins.

In Fig. 13 a similar shape of the detection rate vs. diameter can be recognized. The peak between 4 and 4.5 cm is associated with 1400-km-altitude objects, which are not considered in the model (Fig. 10). Both graphs peak between 3 and 3.5 cm confirming the plausibility of the underlying radar performance model. But the total number of detections is underestimated by a factor of 2.7 at the maxima, requiring an improvement of the model population.

7. CONCLUSIONS

BPE-1/00 was performed successfully delivering reproducible results with respect to previous beam-park exper-

iments. By extending the range window observation of higher orbits was achieved. The comparison with previous experiments revealed the dynamics of the orbital debris environment.

Both orbital debris distribution models evaluated — NASA's Orbital Debris Engineering Model ORDEM2k and ESA's Meteoroid and Space Debris Terrestrial Environment Reference MASTER'99 — underestimate the number of objects significantly, and they miss out the 1400 km altitude orbit. ORDEM2k produces a surface flux table for fixed 50-km-range bins and fixed object size classes leading to ambiguous comparisons with observations. MASTER/PROOF'99 offers many different parameters to compare leading to assumptions on the origin of the differences between the model and the observation. Regarding the general shape of the distributions the model agrees with the observation, therefore, one can assume the radar performance model is plausible, but the observational peaks are mostly underestimated.

8. ACKNOWLEDGEMENTS

The authors are thankful to the TIRA operation crew of FGAN-FHR's Division Radar Techniques for Space Reconnaissance. Their support during the 24-hour experiment made this work possible. The experiment BPE-1/00 was performed and this paper was produced under ESA/ESOC contract no. 13261/98/D/IM(SC).

9. REFERENCES

1. Rosebrock J. et al., Cooperative Debris Tracking and Development of Algorithms for Mid-Size Debris Detection with Radar, *Final Report of ESA/ESOC Study Contracts No. 12248/97/D/IM and No. 12247/97/D/IM*, 201 p., 1999
2. Bendisch J. et al., Extension of ESA's MASTER Model to Predict Debris Detections, *Final Report of ESA/ESOC Study Contract No. 12569/97/D/IM*, 164 p.+ CD-ROM, 2000
3. Leushacke L. et al., Advanced Radar Techniques for Space Debris Observation, *Final Report of ESA/ESOC Study Contract No. 11184/94/D/IM(SC)*, 98 p., 2000
4. Anz-Meandor P., A Decade of Growth, *Orbital Debris Quarterly News*, Vol. 5, No. 4, 2000
5. Settecerri T. et al., Radar Measurements of the Orbital Debris Environment - Haystack and HAX radar, October 1990 – 1998, *NASA report No. JSC 28744*, 1999
6. Jahn R., Comparison of the 1999 Beam-Park Experiment Results with Space Debris Models, *Adv. Space Res.*, in press
7. Bendisch J. et al., Upgrade of ESA's MASTER Model, *Final Report of ESA/ESOC Study Contract No. 12318/97/D/IM*, 267 p. + CD-ROM, 2000
8. Liou J.-C. et al., ORDEM2000's Debris Environment Model, *Orbital Debris Quarterly News*, Vol. 6, NO. 1, 2001